DANMARKS OG GRØNLANDS GEOLOGISKE UNDERSØGELSE RAPPORT 1999/17

EFP-98 Rock physics of Chalk: Analysis of acoustic log data from well MFF-19P, Dan field

ENS J.nr. 1313/98-007

Lars Gommesen & Peter Japsen

GEOLOGICAL SURVEY OF DENMARK AND GREENLAND
MINISTRY OF ENVIRONMENT AND ENERGY

GEUS

DANMARKS OG GRØNLANDS GEOLOGISKE UNDERSØGELSE RAPPORT 1999/17

EFP-98 Rock physics of Chalk: Analysis of acoustic log data from well MFF-19P, Dan field

ENS J.nr. 1313/98-007

Lars Gommesen & Peter Japsen

Released 01.05.2005

GEOLOGICAL SURVEY OF DENMARK AND GREENLAND
MINISTRY OF ENVIRONMENT AND ENERGY

G E U S

Summary

The acoustic and elastic properties of the Tor Formation in well MFF-19P have been studied with respect to the influence of porosity, pore fluid and effective stress. The acoustic properties are found to be influenced by pore fluid and porosity. The V_p-V_s ratio for the Tor Formation clearly reflects whether the pore fluid is oil or brine, and porosity is found to correlate with both V_p and V_s, impedance and bulk modulus. Fluid substitution has been performed, and linear average trends have been established between porosity and V_p, V_s and impedance for the Tor Formation saturated with brine. The acoustic properties are unaffected by variations in effective stress over the studied interval.

Introduction

This report is part of the EFP-98 project Rock Physics of Chalk, and presents the results of the analysis of the acoustic log data measured in well MFF-19P. The report focuses on the acoustic and elastic properties of the Tor Formation, but data from the Ekofisk formation are included for comparison.

The study of the acoustic and the elastic properties of the Tor and Ekofisk formations is primarily based on the acoustic response recorded by the DSI log (Dipole Sonic Imager). Whereas the acoustic properties are studied directly from the measured compressional and shear waves velocities (V_p and V_s), the elastic properties are based on the dynamic, elastic moduli. These moduli are calculated from acoustic (DSI) and density log data.

In carbonate rocks the compressional wave and shear wave velocities are mainly controlled by porosity. Several other intrinsic and extrinsic parameters influence the acoustic properties of the rock. The first group of parameters includes fluid type, texture, and lithology, whereas the latter group includes effective stress and wave frequency. The influence of porosity, pore fluid, and effective stress are analysed with respect to rock physics theory and by the use of the PetroTools software.

Formations and zones

The Tor and Ekofisk formations of the Chalk Group are both represented in well MFF-19P. Within the Chalk Group, the Danian Tight Zone and the Upper Maastrichtian are recognised (Table 1). Note that base Upper Maastrichtian is not recognised. The total studied interval of well MFF-19P is from top chalk to maximal depth of the log suite.

Formation	*Recognised tops*	*MDKB [ft]*	*TVDSS[ft]*	*TVDSS [m]*
Ekofisk	Top chalk	8608	-6211	-1893
Ekofisk	Danian Tight	8733	-6270	-1911
Tor	Upper Maastrichtian	8850	-6325	-1928
max depth	-	10500	-7231	-2204

Table 1. Stratigraphy of the logged chalk interval of well MFF-19P. Depth top zones are given.

Logs and control parameters

Several logs have been used in this study (Table 2). All logs are correlated by depth and given by MDKB, TVDKB, TVDSS (see Parameters for description of logs). All data of the mentioned logs are included in the analysis and no data has been edited or deleted except bad data of depth interval (8845.5; 8846.5 ft MDKB).

Log name	*Origin*
VCA	1-VSHmin, see text below.
VSHmin	GEUS.
DTCO	Mærsk (Schlumberger).
DTSH	Mærsk (Schlumberger).
Eff_stress	See Effective stress.
PHI_e	GEUS.
RHOb_e	GEUS.
SONIC	Mærsk (Schlumberger).
So	1-Sw, see text below.
Sw	GEUS.
Temp	Mærsk (Schlumberger).

Table 2. Logs used as input for the acoustic study.

The mineralogical composition of the reservoir rock is simplified to be composed only by chalk and clay. Thus one minus clay content is calculated to be equal to chalk content. Also the fluid composition of the reservoir fluid is simplified to be composed only by brine and oil, therefore one minus water saturation is calculated to be equal to the oil saturation.

Synthetic density and velocity logs for solids and fluids are generated in PetroTools on basis of the logs in Table 2 and control parameters defined in PetroTools (Table 3). The velocity logs representing the solid phase ($V_{p,solid}$ and $V_{s,solid}$) are calculated on basis of the control parameters of calcite and clay (shear and bulk modulus) and the volume fractions of these two minerals. The $V_{p,solid}$ and $V_{s,solid}$ are hereby estimated independent from porosity. PetroTools generate the effective moduli of a multiphase (here a two-phase) composite by the use of the Voigt-Reuss-Hill average (Equation 1).

Equation 1

$$M_{Voigt\,ReussHill} = \frac{M_{Voigt} + M_{Reuss}}{2},$$

Equation 2

$$M_{Voigt} = \sum_{i=1}^{N} f_i M_i,$$

Equation 3

$$\frac{1}{M_{Reuss}} = \sum_{i=1}^{N} \frac{f_i}{M_i},$$

where f_i and M_i are the volume fraction and modulus of the i´th component, respectively (Mavko et al., 1998).

The $V_{p,fluid}$ log is based on density, bulk modulus and V_p of the components of the fluid (here oil and brine). Here the effective bulk modulus of a homogeneous fluid K_{fluid} is calculated from Reuss average (Equation 3). The respective acoustic properties of each of the components of the fluid are based on empirical results summarised by Batzle and Wang (1992) and is controlled by the fluid builder parameters of Table 3. Control parameters, used in the PetroTools constant manager. Here subdivided by subject. as a function of pressure and temperature.

The effective density of respectively solid and fluid are calculated as:

Equation 4

$$\rho_{eff} = \sum_{i=1}^{N} f_i \rho_i,$$

where f_i and ρ_i are the volume fraction and density of the i´th component, respectively.

Subject	Parameter	Value
Fluid builder	NaCl Sal	100000 ppm
	GOR	1100 scf/bbl
	Oil gravity	30 API
	Gas gravity	0.5 (specific)
	Gas index (brine; oil)	0; 0
Fluids	Brine (ρ; K)	1010 kg/m^3; 2.25 GPa
	Oil (ρ; K)	755 kg/m^3; 1.30 GPa
Mineralogy	Calcite (ρ; K; G)	2710 kg/m^3; 76.8 Gpa; 32 GPa
	Clay (ρ; K; G)	2580 kg/m^3; 32.0 GPa; 6.85 GPa

Table 3. Control parameters, used in the PetroTools constant manager. Here subdivided by subject.

Effective stress

The effective in situ stress in the formation at a specific depth is calculated from the effective overburden stress gradient and a reservoir pore pressure gradient. The pore pressure gradient vary through the studied interval, due to differences in the composition of the reservoir fluid (here assumed to be an idealised mix of oil and brine). The general, initial reservoir pore pressure at the Dan Field is given as 3820 psi at - 6060 ft TVDSS (Mærsk Oil & Gas A/S, 1989). An initial pore pressure at top chalk in well MFF-19P (-6211 ft TVDSS) is calculated in Equation 5 under the assumption, that the top chalk pore fluid is characterised by a gradient on 0.44 psi/ft. Based on this initial pressure, the reservoir pore pressure is calculated from the fluid gradients given in Table 5 and the idealised fluid composition illustrated in Figure 1. As example the calculated pore pressure for the depth interval –6211; -6400 ftTVDSS is given in Equation 6.

Equation 5.

$$P_{pore} = 3820 psi + (6211 ft - 6060 ft) * 0.44 psi / ft = 3887 psi$$

Equation 6.

$$P_{pore} = P_{p,datum} + (|z| + datum) * (S_w * 0.44 psi / ft + (1 - S_w) * 0.33 psi / ft) \Leftrightarrow$$
$$P_{pore} = 3887 psi + (|z| - 6211 ft) * 0.385 psi / ft,$$

where $P_{pore,datum}$ is 3887 psi, *datum* is -6211 ft, TVDSS, $S_w=0.5$, $1-S_w=S_o$, and z is numeric depth in ft, TVDSS. Note in the two following intervals (b and c) of Figure 1 ($P_{pore,datum}$, *datum*)-values are approximately (3959 psi, -6400 ft) and (3994 psi, -6500 ft).

The effective stress is calculated as external stress subtracted pore pressure. Since the sea depth is 140 ft and the overburden and the gradients are given in Table 5 (seawater and brine gradient is assumed identical), the effective stress can be calculated as:

Equation 7.

$$\sigma_{eff} = \left((z - 140ft) * 0.9psi/ft + 140ft * 0.44psi/ft\right) - P_{pore},$$

where P_{pore} is calculated from Equation 6.

Type of gradient	*psi/ft*	*kPa/m*
Overburden gradient	0.90	20.25
Oil gradient	0.33	7.43
Brine gradient	0.44	9.90

Table 5. Gradients used to calculate effective stress in the formation (Engstøm, personal communication 1999; Japsen, 1998). Seawater and brine gradient is assumed identical.

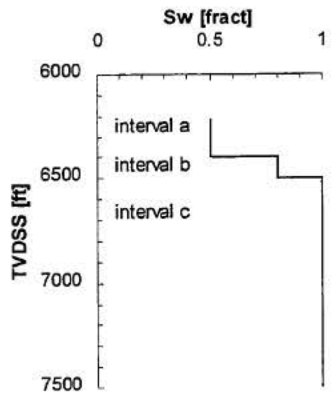

Figure 1. Idealised fluid composition of the studied well interval (S_o = *1* - $S_{w,idealised}$). The idealised fluid composition is only used for effective stress estimating.

Acoustic and elastic properties

The acoustic and elastic properties are here studied with respect to depth, effective stress, pore fluid, and porosity.

Acoustic properties versus extrinsic parameters

Depth and stress. Plots of V_p & V_s, V_p/V_s versus depth and V_p, V_s versus effective in situ stress are given in Appendix 1 as Figure 2, Figure 3, and Figure 4 (respectively). From Figure 2 it is observed, that the compressional and shear velocities of the Tor Formation correlate with depth from OWC and downwards. The V_p and V_s of this interval are almost constant with average values around 3785 m/s and 1960 m/s, respectively. In the upper Tor interval (above OWC) it is observed, that the variations in V_s values are not of such magnitude as the variations in V_p values. This is also observed from the V_p and V_s values of the Ekofisk Formation.

Figure 3 summarise the magnitude variations of V_p and V_s with depth. The V_p/V_s ratio versus depth show a change in magnitude of V_p/V_s ratio atthe OWC. From OWC down to –7060 ft, TVDSS the V_p/V_s is constant with an average of 1.94. From this depth an downward the ratio seems to decrease to a value clearly below 1.9 (indicated by a blue arrow signature at the figure). From the OWC up to the change of formation, the V_p/V_s ratio exceeds a relatively low value, with an average ratio of 1.84. Large variations in the V_p/V_s ratio is observed for the Ekofisk Formation.

From Figure 4 it can be concluded, that there is no significant influence of the effective stress on the acoustic properties in the studied interval, since the acoustic properties from OWC and downwards are almost constant. The variation in the acoustic properties of the studied interval are – as described in the next section – coursed by influence of intrinsic parameters.

Acoustic and elastic properties versus intrinsic parameters

Pore fluid. Variations in V_p/V_s ratios can be induced by variation in pore fluid. A comparison of the V_p/V_s ratio of Figure 3 with S_w of Figure 5 shows a correlation between V_p/V_s and fluid composition from top chalk and downward. An exception, is the anomaly around depth –7200 ft, TVDSS.

The general correlation between V_p/V_s and brine saturation is illustrated in Figure 6. Here the Tor Formation data correlates relatively better than the Ekofisk Formation data. Close to 100% brine saturation a relatively wide range of V_p/V_s values is observed. Since the scatter of brine zone data "covers" the anomaly in this plot, the wide range can not be explained only by the anomaly mentioned above.

V_p/V_s versus porosity (Figure 7) shows no correlation between the two parameters for data of respectively the brine zone and hydrocarbon zone. As for Figure 6, the Ekofisk Formation data scatter relatively more than Tor Formation data.

The V_p/V_s independence of porosity can be explained by the strong correlation between the V_p and V_s velocities and porosity. This relationship can for the Tor Formation data be observed in Figure 8, where linear correlation trends are included. The increase in velocity due to decrease in porosity is lower than estimated by Raiga-Clemenceau *et al.* (1988), who generally overestimate V_p (Figure 10). The velocity plotted versus velocity estimated by Wyllie *et al.* (1956) shows that the V_p of the brine zone is relatively well estimated, whereas the V_p of the hydrocarbon zone is underestimated. Note, that the input parameters of Wyllie´s equation (V_{fluid} and $V_{s,solid}$) is based on the simplified compositions of fluid and mineralogy (see Logs and control parameters). For the Ekofisk Formation data correlation between velocity and porosity is also observed although correlation is not as strong as for the Tor Formation. Also note that even though that a linear correlation is included in the velocity-porosity plot of Figure 8, such relationship is not expected to be linear for a wide porosity interval.

The V_p, V_s plot of Figure 12 shows a strong correlation between the compressional and shear velocity for data of the Tor Formation. The low velocity (high porosity) data of the hydrocarbon zone deviates slightly from the brine zone data. As observed, the Ekofisk Formation data correlates, but does not continue the V_p,V_s trend of the Tor brine zone data. As for the velocity, porosity plot of Figure 9 the impedance-porosity plot of Figure 13 shows strong correlation for the Tor formation data and a weaker correlation for the Ekofisk Formation data. The increase in impedance due to lower porosity is of larger magnitude for the Tor Formation compared to the Ekofisk Formation.The elastic properties can be evaluated on basis of the elastic moduli, which is defined on the principles of Hooke's law and from the assumption, that the rock behave as a linear elastic material. Here, the elastic moduli are expressed from a dynamic viewpoint. Rock material responds to time harmonic external stress (or strain) induced by sound waves propagating through rock. This response is controlled by elastic stiffness and rock density, which means that the elastic moduli can be expressed from sound velocities and rock densities. In Figure 14 and Figure 15 respectively the bulk modulus and Poisson´s ratio is plotted versus porosity. As expected, bulk modulus shows dependence of porosity and Poisson´s ratio does not. Note, the variation in magnitude of Poisson´s ratio is controlled by the pore fluid composition.

In Equation 8 and Equation 9 bulk modulus (K) and Poisson´s ratio (ν) is defined from a dynamic viewpoint. Note, that when two elastic moduli are known it is possible to calculate other elastic moduli.

Equation 8

$$K = \rho\left(Vp^2 - \tfrac{4}{3}Vs^2\right),$$

Equation 9

$$\nu = \frac{Vp^2 - 2Vs^2}{2(Vp^2 - Vs^2)},$$

where ρ is bulk density.

Fluid substitution

When comparing acoustic log data of different origin it is often useful to substitute from original fluid to e.g. brine to eliminate the fluid effect on acoustic properties.

The theory of fluid substitution based on Gassmann (1951)- Biot (1956) relations is resumed by Mavko *et al.* (1998), who is cited in the following:

Generally, when a rock is loaded under an increment of compression, such as from a passing seismic wave, an increment of pore pressure change is induced, which resists the compression and therefore stiffens the rock. The low-frequency Gassmann (1951)-Biot (1956) theory predicts the resulting increase in effective bulk modulus, K_{sat}, of the saturated rock through the following equation:

Equation 10

$$\frac{K_{sat}}{K_0 - K_{sat}} = \frac{K_{dry}}{K_0 - K_{dry}} + \frac{K_{fl}}{\varphi(K_0 - K_{fl})},$$

$$\mu_{sat} = \mu_{dry},$$

where

- K_{dry} = *effective bulk modulus of dry rock*
- K_{sat} = *effective bulk modulus of the rock with pore fluid*
- K_0 = *bulk modulus of mineral material making up rock*
- K_{fl} = *effective bulk modulus of pore fluid*
- φ = *porosity*
- μ_{dry} = *effective shear modulus of dry rock*
- μ_{sat} = *effective shear modulus of rock with pore fluid*

Gassmann´s equation assumes a homogeneous meniral modulus and statistical isotrophy of the pore space but is free of assumptions about the pore geometry. Most importantly, it is valid only at sufficiently ***low frequencies*** *such that the induced pore pressures are equilibrated throughout the pore space (i.e., there is sufficient time for the pore fluid to flow and eliminate wave-induced pore pressure gradients). This limitation to low frequencies explains why Gassmann's relation works best for very low frequency in situ seismic data (<100 Hz) and may perform less well as frequencies increase toward sonic logging ($\approx 10^4$Hz) and laboratory ultrasonic measurements ($\approx 10^6$Hz).*

A substitution of the present fluid with brine is performed by the use of PetroTools, which is based on the theory just described (note, it is not correct just to replace K_{dry} in Equation 10 by $K_{new\ fluid}$). The theory above does not predict any change in shear modulus due to saturation, since there is no change in the net volume associated with shear deformations in an isotropic rock and therefore no compression of the pore fluid.

In PetroTools the bulk and shear modulus is calculated from V_p, V_s, and ρ (from a dynamic viewpoint), then the bulk modulus is transformed to represent the rock saturated with the new fluid, and then the new velocities corresponding to the change in modulus is calculated. The bulk density that is used in the velocity-moduli relations is given by Equation 4 and calculated from ρ_0, ρ_{fl}, and φ.

In Appendix 3 all figures represent either the acoustic or elastic responses of the rock saturated with the new, substituted fluid. The control parameters of the new fluid (100 % brine) are given in Table 3.

Figure 16 illustrates the new V_p and the V_s responses versus depth compared to the original response. As observed the V_p increases significantly in the hydrocarbon zone due to the increase in effective bulk modulus. The increase in fluid bulk modulus has stronger influence on the effective modulus than the increase in density. In contrast, the V_s theoretically decreases slightly because of an increase in density and a constant shear modulus.

In Figure 17 the V_p/V_s ratio has increased to a value above 2.0, which is significantly higher than the ratio of the original brine zone. This can be explained by an overestimation of the bulk modulus for brine or an underestimation of the brine density (see control parameters in Table 3). The V_p/V_s, porosity plot of Figure 18 shows, that the high porosity data of the Tor Formation now exceeds at value around 2.0 compared to the original, which was approximately 1.84.

Strong correlation is observed between velocity and porosity, when data are plotted in as in Figure 19. The new linear average trends, shows relatively lower increase in velocity due to decrease in porosity when the trends are compared to the original trends. Note, that the shear velocity trend is almost unaffected of the fluid substitution.

Strong correlation is also observed for the V_p, V_s plot of Figure 20 and the impedance, porosity plot of Figure 21. The observed increase in impedance, due to porosity decrease, is lower for the modelled data of Figure 21 compared to the original data.

The elastic moduli of Figure 22 and Figure 23 illustrates respectively the correlation between bulk modulus and porosity and a constant Poisson´s ratio for Tor Formation chalk saturated with brine.

Discussion and conclusion

The acoustic and elastic properties of the Tor Formation of well MFF-19P has been studied with respect to the influence of effective stress, porosity, pore fluid.

Down through the depth interval of the Tor Formation, the effective stress increases from approximately 11.7 to 14.7 MPa. In this interval no increase in velocity due to increase in stress has been observed. When stress is constantly increased, the stress induced increase in velocity is expected to decrease. For the Tor Formation data, the observed independence between acoustic properties and effective stress therefore might be explained by the combination of a relatively high magnitude of the effective stress combined with a relatively small increase in stress.

Porosity and pore fluid influence on the acoustic and elastic properties of the studied chalk. The V_p/V_s ratio eliminates the strong influence of porosity and thus used for studying the influence of pore fluid. A significant difference between the acoustic properties of hydrocarbon saturated chalk and brine saturated chalk is hereby found. An average ratio of the hydrocarbon zone is approximately 1.84, whereas the ratio of the brine zone exceeds a value of approximately 1.94.

Porosity is found to correlate with both compressional and shear wave velocity- impedance and bulk modulus. For the studied porosity interval (approximately 17%; 36%) linear average trends for the Tor Formation saturated with brine is found. The trends of V_p, V_s, and I are based on 3396 data points which has undergone a Biot-Gassmann fluid substitution (Equation 11 to Equation 13).

Equation 11

$$V_p = -74\varphi + 5528,$$
$$R^2 = 0.80$$

Equation 12

$$V_s = -29\varphi + 2647,$$
$$R^2 = 0.76$$

Equation 13

$$I = V_p\rho = -0.23\varphi + 14.1,$$
$$R^2 = 0.88$$

where φ is given in %, velocity is given in m/s and I is given in 10^6*kg/m^3*m/s.

The performed fluid substitution seems to overestimate the acoustic response in the original hydrocarbon zones. It is likely, that this can be explained by a bulk modulus of the brine that is too high.

Parameters

DTCO	Delta-T (travel time) compressional wave. DSI tool.
DTSH	Delta-T (travel time) shear wave. DSI tool.
Eff_stress	Effective in situ stress calculated in paragraph Effective stress.
GOR	Gas oil ratio.
I	Impedance calculated from density and compressional velocity.
MDKB	Measured depth from KB.
NaCl Sal	Salinity.
OWC	Oil water contact.
PHI_e	Interpreted porosity. Bore hole environment corrected.
RHO_e	Interpreted bulk density. Bore hole environment corrected.
KB	Kelly bushing.
ρ_{fl}	Density of pore fluid.
ρ_0	Density of the mineral that builds the rock.
Solid	The effective rock building mineral composition.
SONIC	Delta-T (travel time) compressional wave. Sonic tool.
S_o	Oil saturation.
S_w	Brine saturation.
Temp	Temperature.
TVDKB	True vertical depth from KB.
TVDSS	True vertical depth from mean sea level (positive above sea level).
VCA	Volume calcite.
VSHmin	Volume shale, from gamma ray log.
V_p	Compressional velocity.
V_s	Shear velocity.

References

Batzle, M., and Wang, Z., 1992. Seismic properties of pore fluids. *Geophysics*, 57, 1396-1408.

Biot, M. A.,1956.Theory of propagation of elastic waves in a fluid saturated porous solid. I. Low frequency range and II. Higher-frequency range. *J. Acoust. Soc. AM.*, 28, 168-191.

Gassmann, F., 1951. Elastic waves through a packing of spheres, *Geophysics*, 16, 673-685.

Japsen, P., 1998. Regional Velocity-Depth Anomalies, North Sea Chalk: A Record of Overpressure and Neogene Uplift and Erosion, *AAPG Bulletin*, 82, 2031-2074.

Mavko, G., Mukerji, T., Dvorkin, J., 1998. *The Rock Physics Handbook*, The Press Syndicate of the University of Cambridge, United Kingdom.

Mærsk Oil & Gas A/S, 1989. *Dan Petrophysical Review*, Vol. 1., March.

Raiga-Clemenceau, Martin, J., P., and Nicoletis, S., 1988. The concept of acoustic formation factor for more accurate porosity determination from sonic transit time data, *The Log Analyst*, 29, 54-60.

Wyllie, M. R. J., Gregory, A. R., and Gardner, L. W., 1956. Elastic wave velocities in hetrogeneous and pouros media, *Geophysics*, 21, 41-70.

Appendix 1

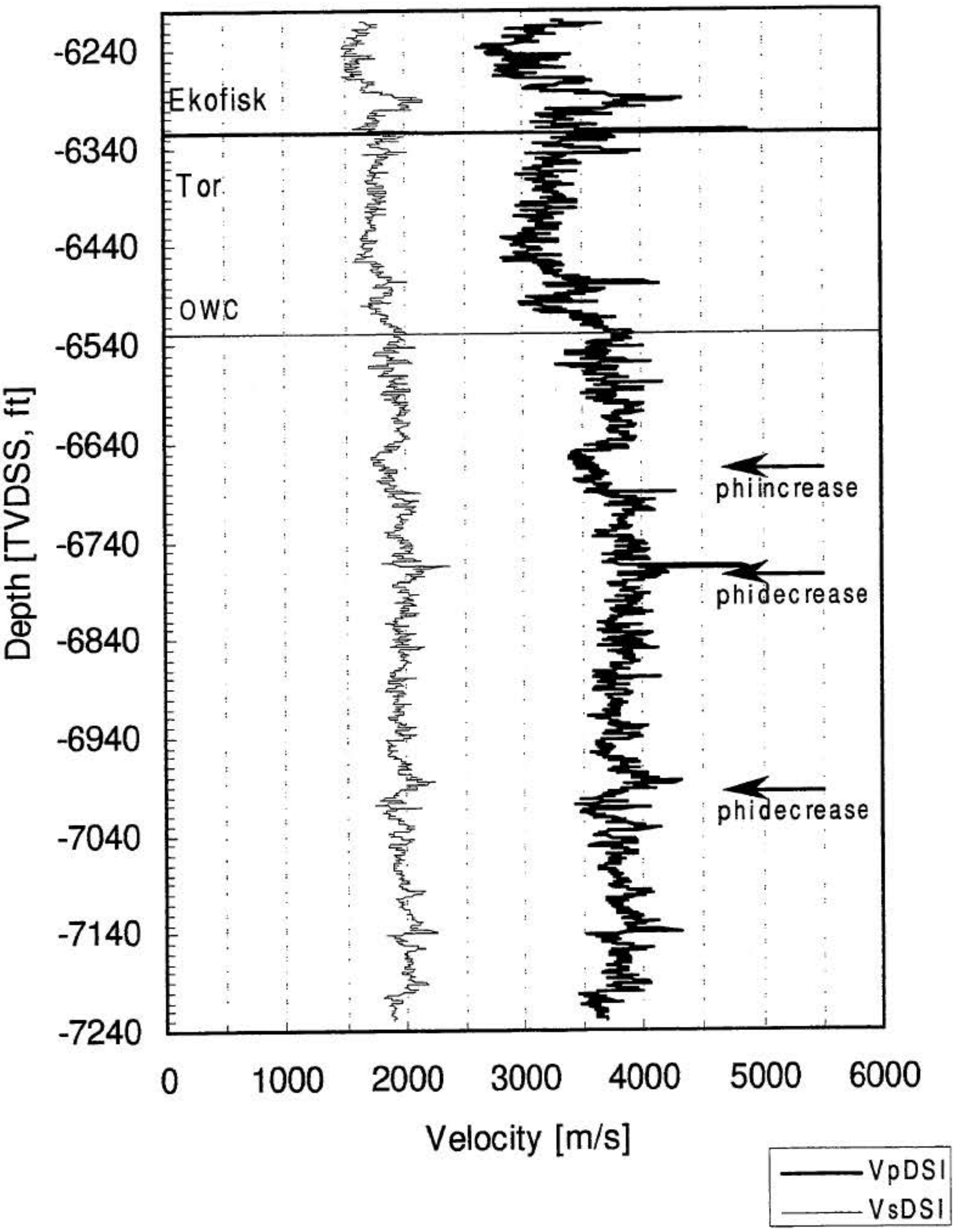

Figure 2. V_p and V_s vs. depth for well MFF-19P. Variations in the brine zone interval, which reflects (larger) variations in porosity, is included (blue arrow signature).

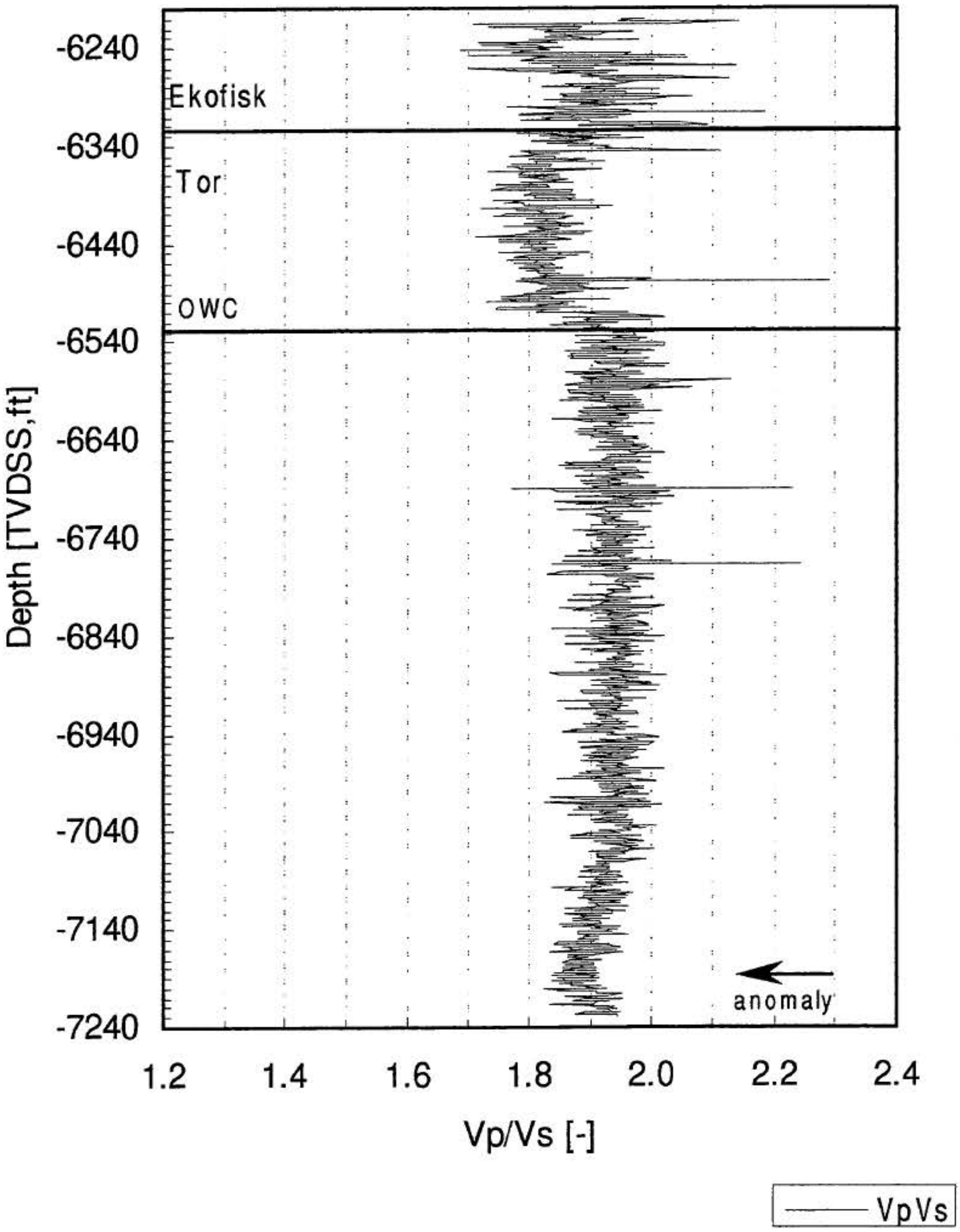

Figure 3. V_p/ V_s vs. depth for well MFF-19P. Anomaly, which not reflects change in pore fluid, is included (blue arrow signature).

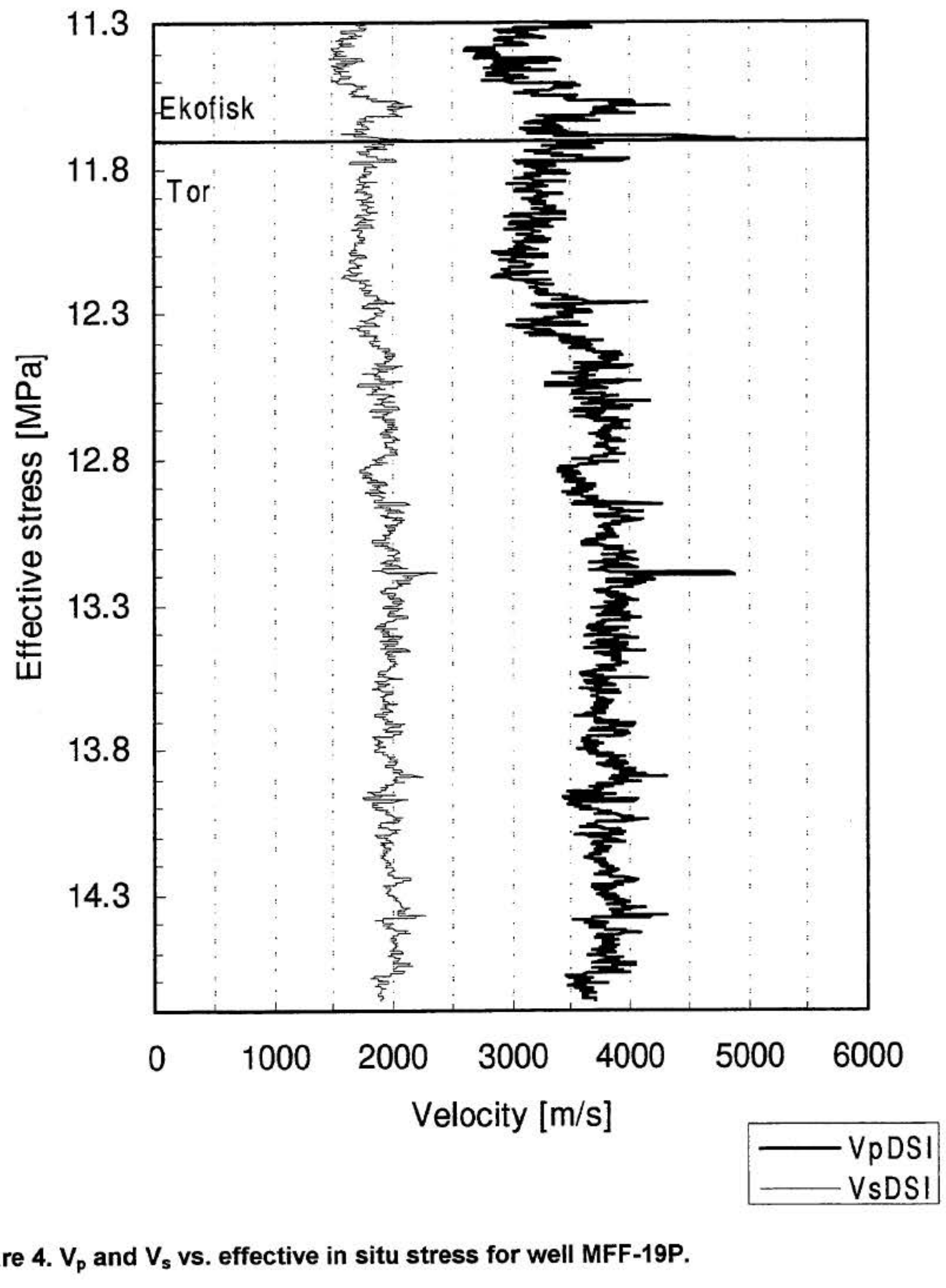

Figure 4. V_p and V_s vs. effective in situ stress for well MFF-19P.

Appendix 2

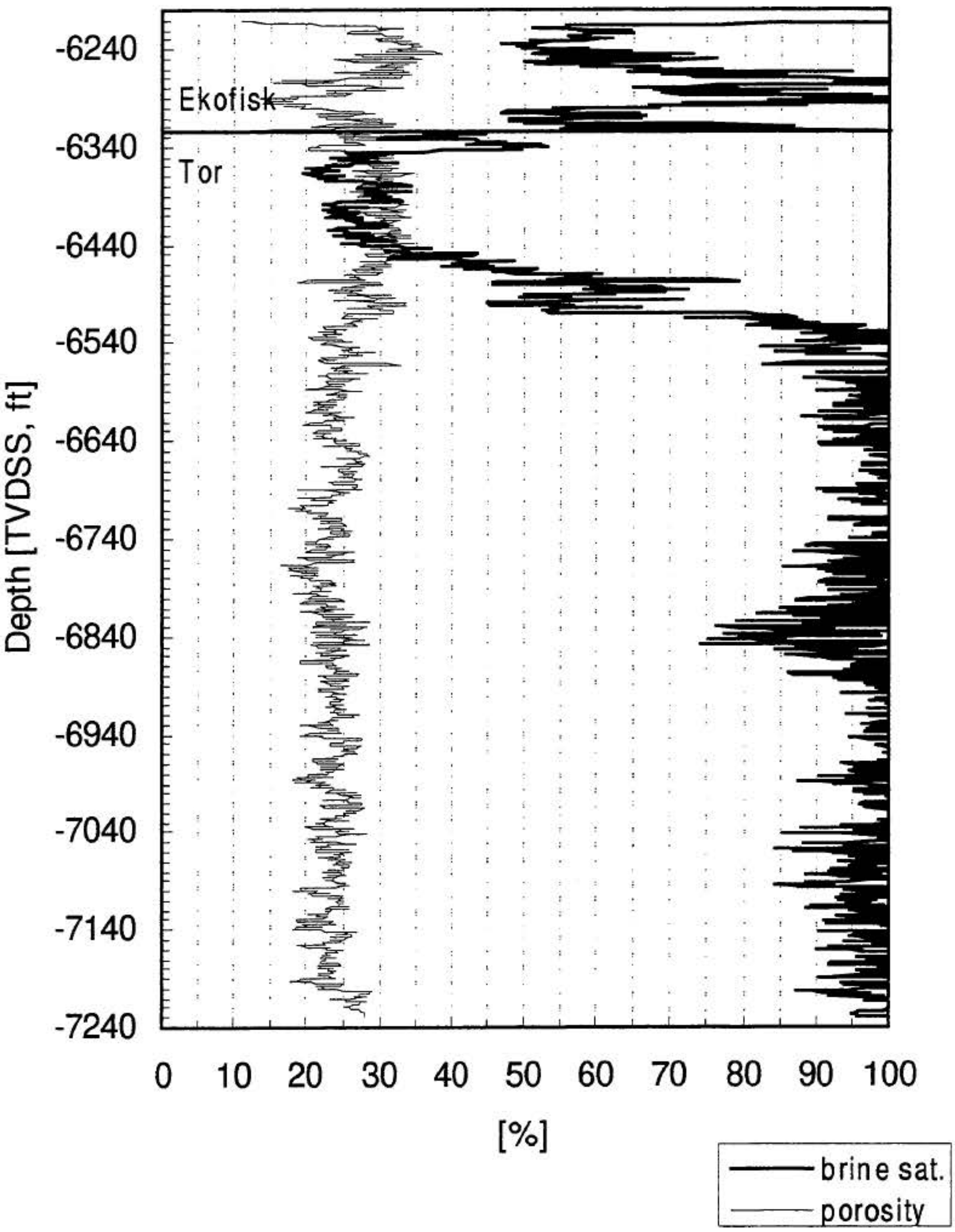

Figure 5. Brine saturation and porosity vs. depth for well MFF-19P.

(Appendix 2 continued)

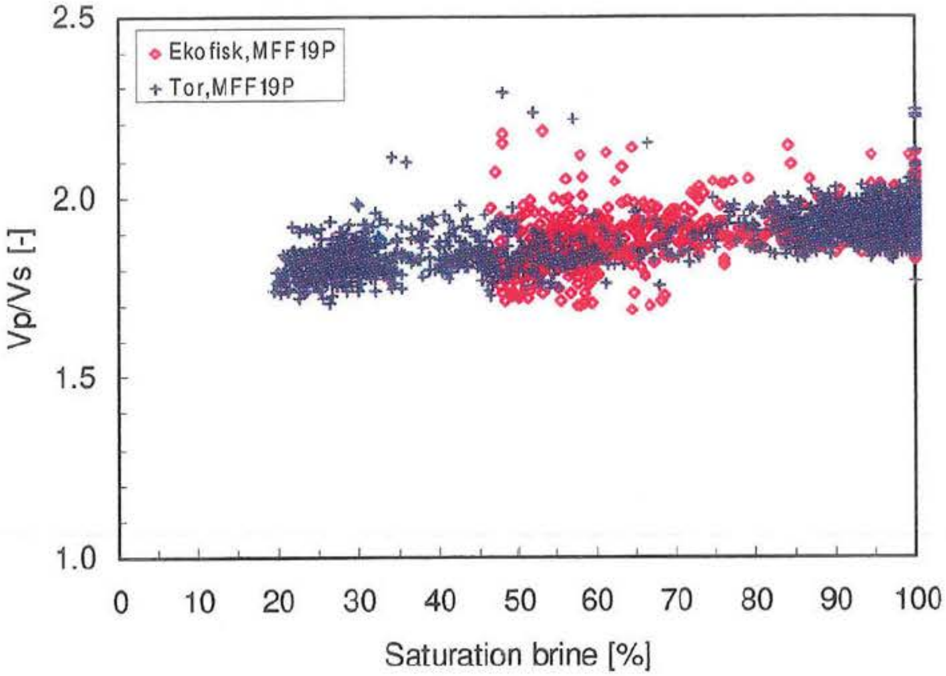

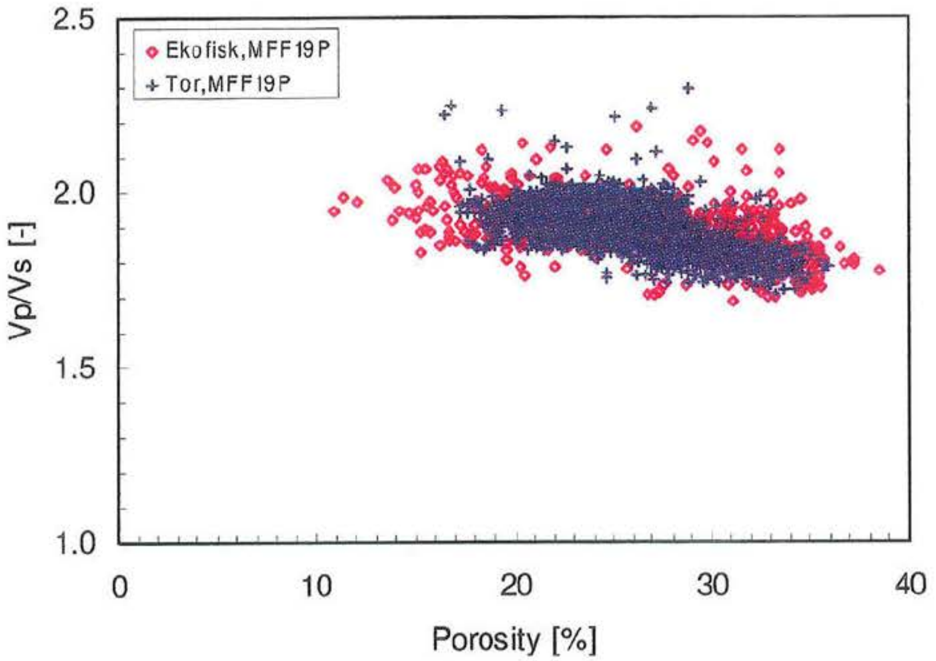

Figure 6 (top). V_p/V_s vs. brine saturation for Tor and Ekofisk Formation, well MFF-19P [no. of data points 3396 (Tor), 486 (Ekofisk)].

Figure 7 (bottom). V_p/V_s vs. porosity for Tor and Ekofisk Formation, well MFF-19P [no. of data points 3396(Tor), 486(Ekofisk)].

(Appendix 2 continued)

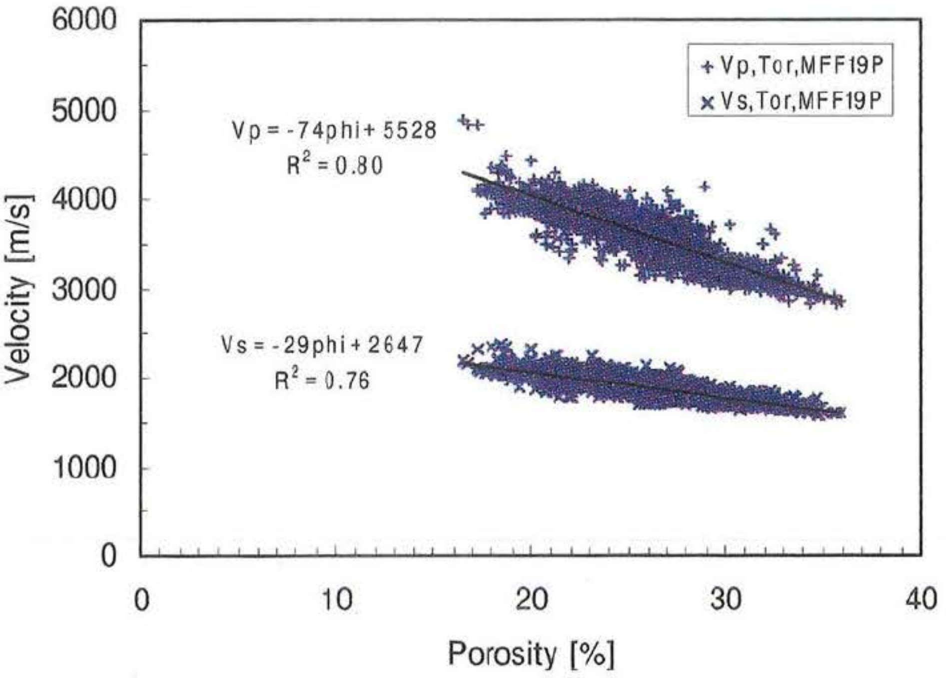

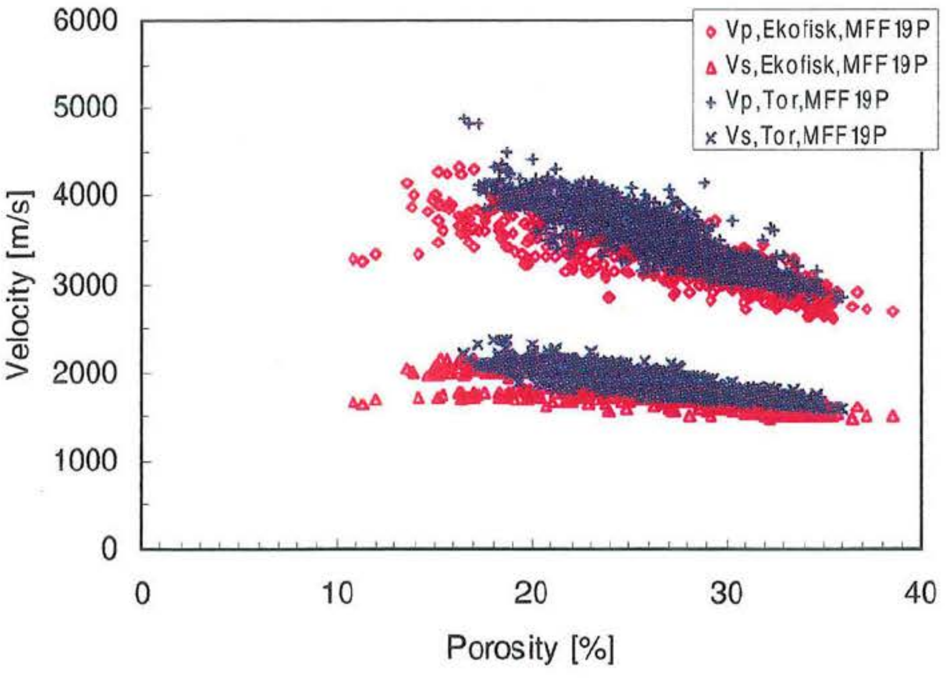

Figure 8 (top). V_p and V_s vs. porosity for Tor Formation data, well MFF-19P [no. of data points: 3396].

Figure 9 (bottom). V_p and V_s vs. porosity for Tor and Ekofisk Formation data, well MFF-19P [no. of data points: 3396(Tor), 484(Ekofisk)].

(Appendix 2 continued)

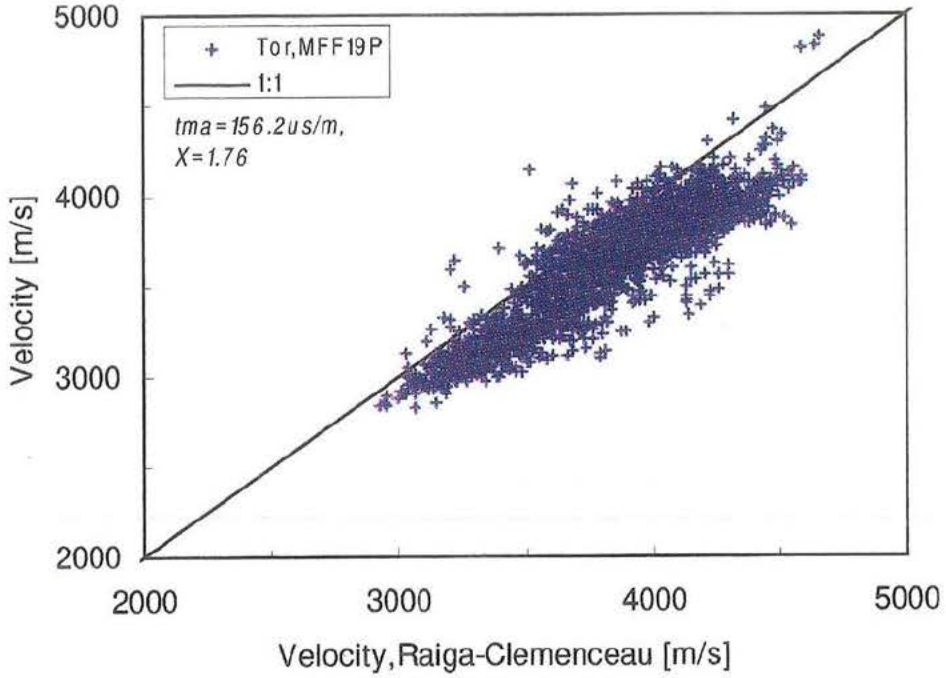

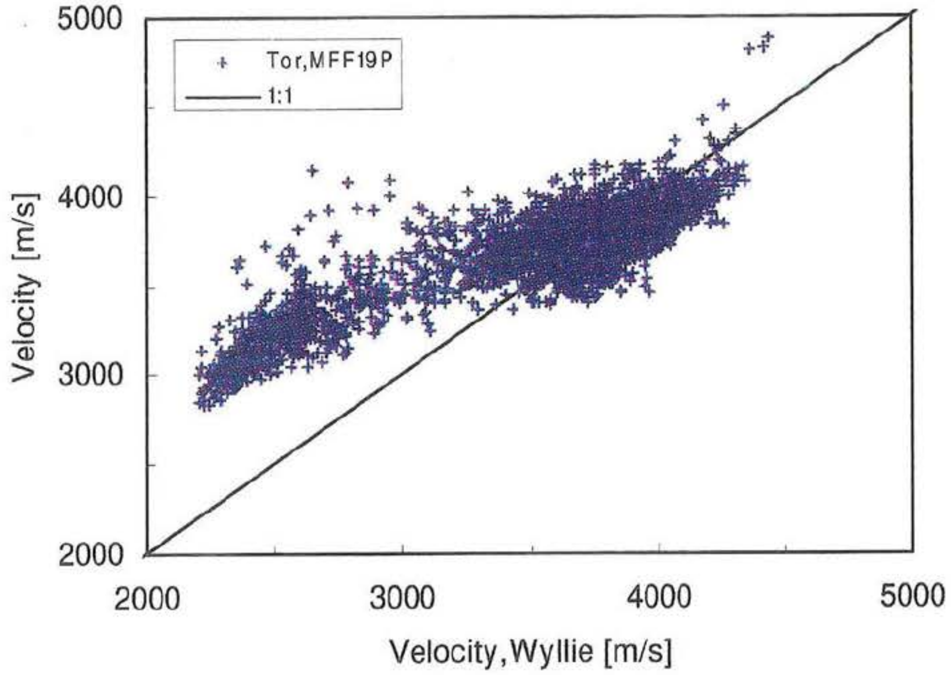

Figure 10 (top). V_p vs. estimated velocity (Raiga-Clemenceau *et al.*, 1988) [no. of data points: 3396].

Figure 11(bottom). V_p vs. estimated velocity (Wyllie *et al.*, 1956) [no. of data points: 3396].

(Appendix 2 continued)

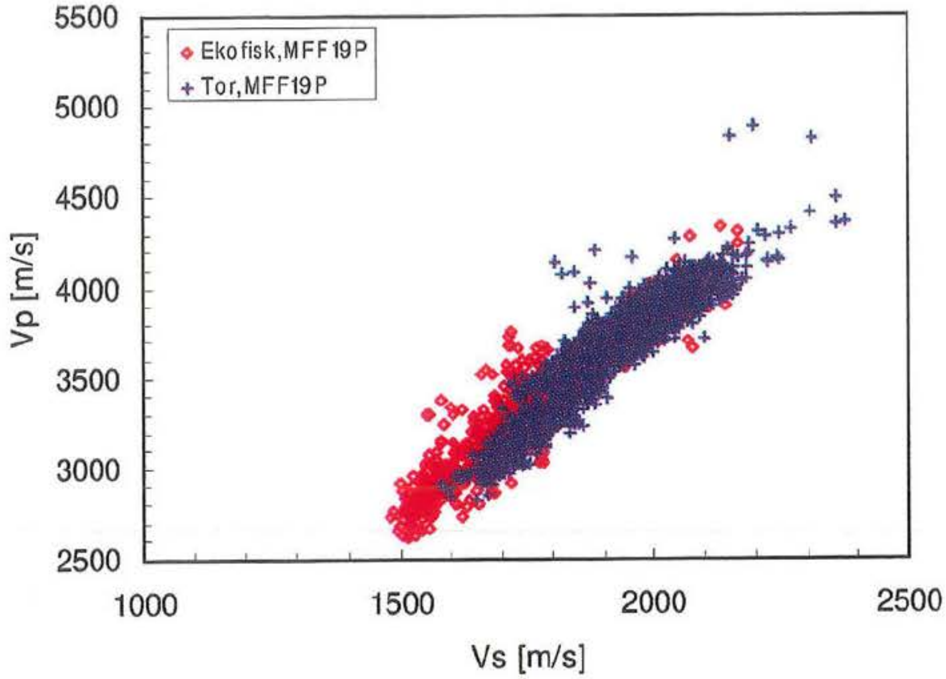

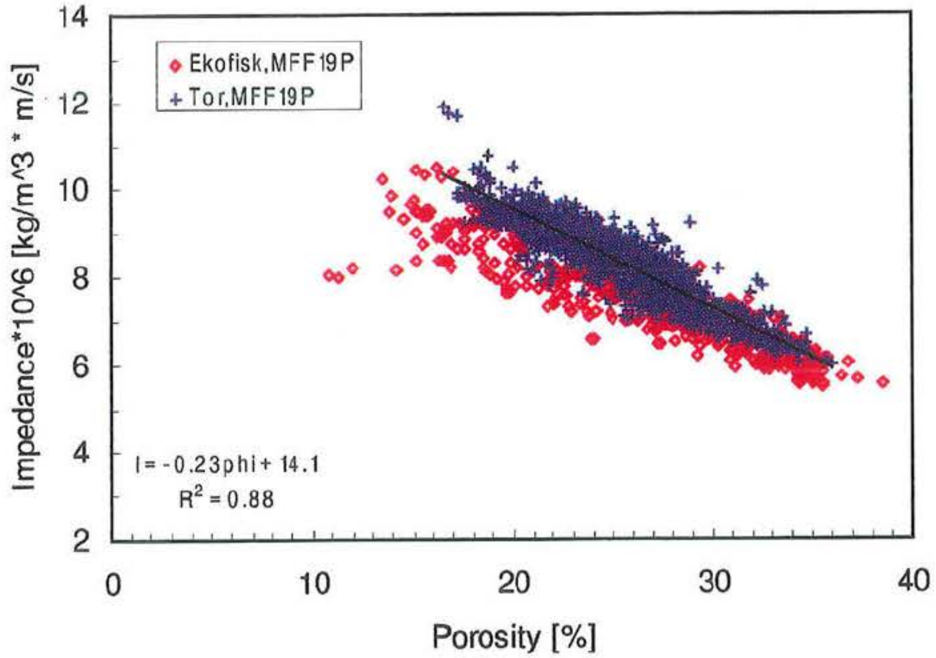

Figure 12 (top). V_p vs. V_s for Tor and Ekofisk Formation, well MFF-19P [no. of data points: 3396 (Tor), 486 (Ekofisk)].

Figure 13 (bottom). Impedance (V_p *ρ) vs. porosity for Tor and Ekofisk Formation, well MFF-19P [data points: 3396 (Tor), 486 (Ekofisk)]. Linear Tor trend included.

(Appendix 2 continued)

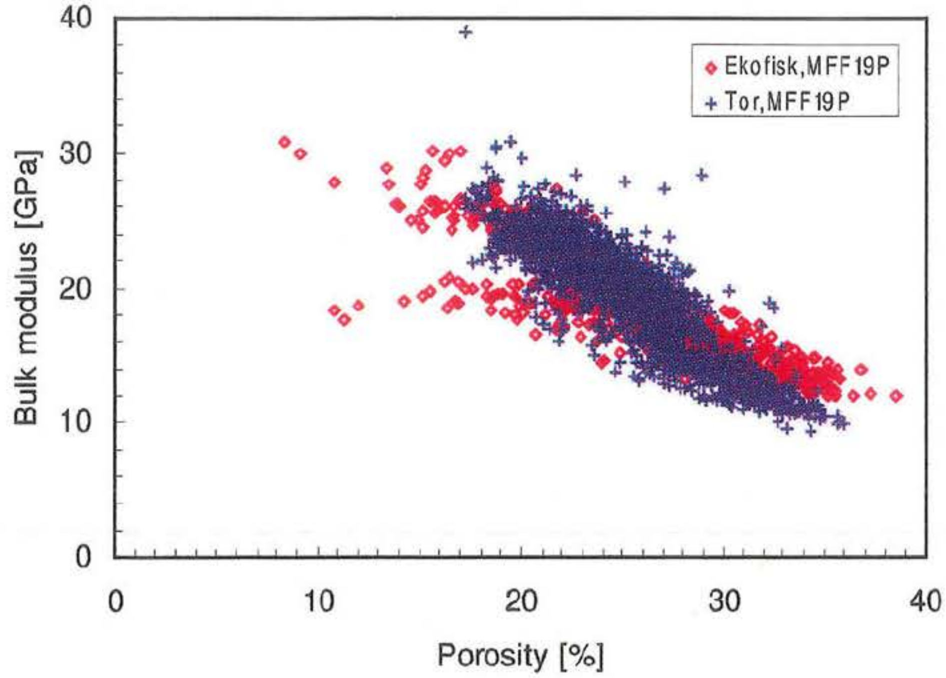

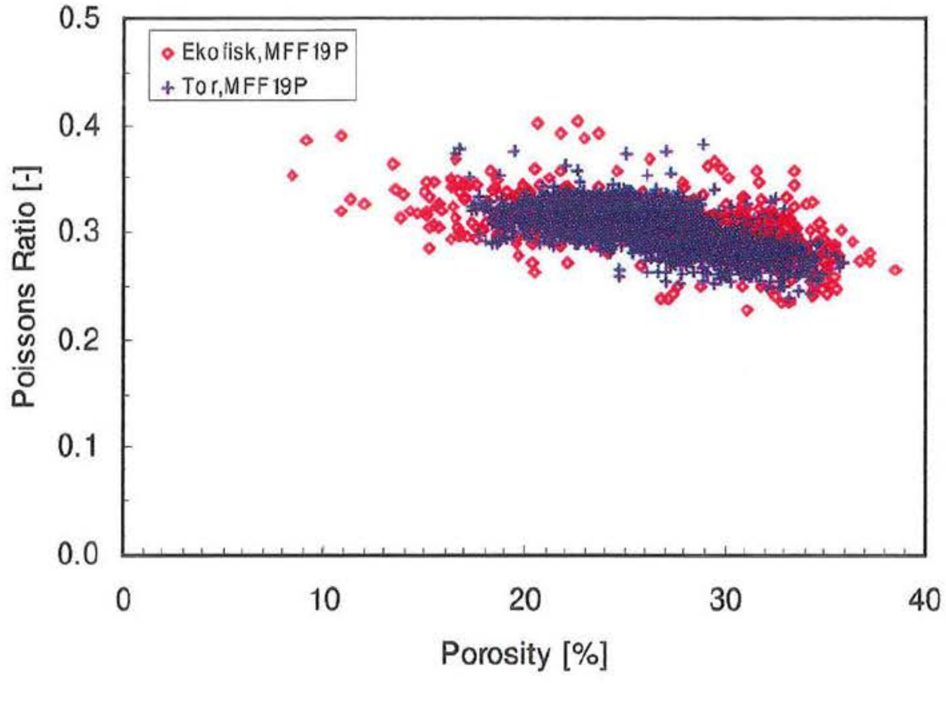

Figure 14 (top). Bulk modulus vs. porosity for Tor and Ekofisk Formation, well MFF-19P [no. of data points: 3396(Tor), 484(Ekofisk)].

Figure 15 (bottom) Poisson´s ratio vs. porosity for Tor and Ekofisk Formation, well MFF-19P [no. of data points: 3396 (Tor), 484 (Ekofisk)].

Appendix 3

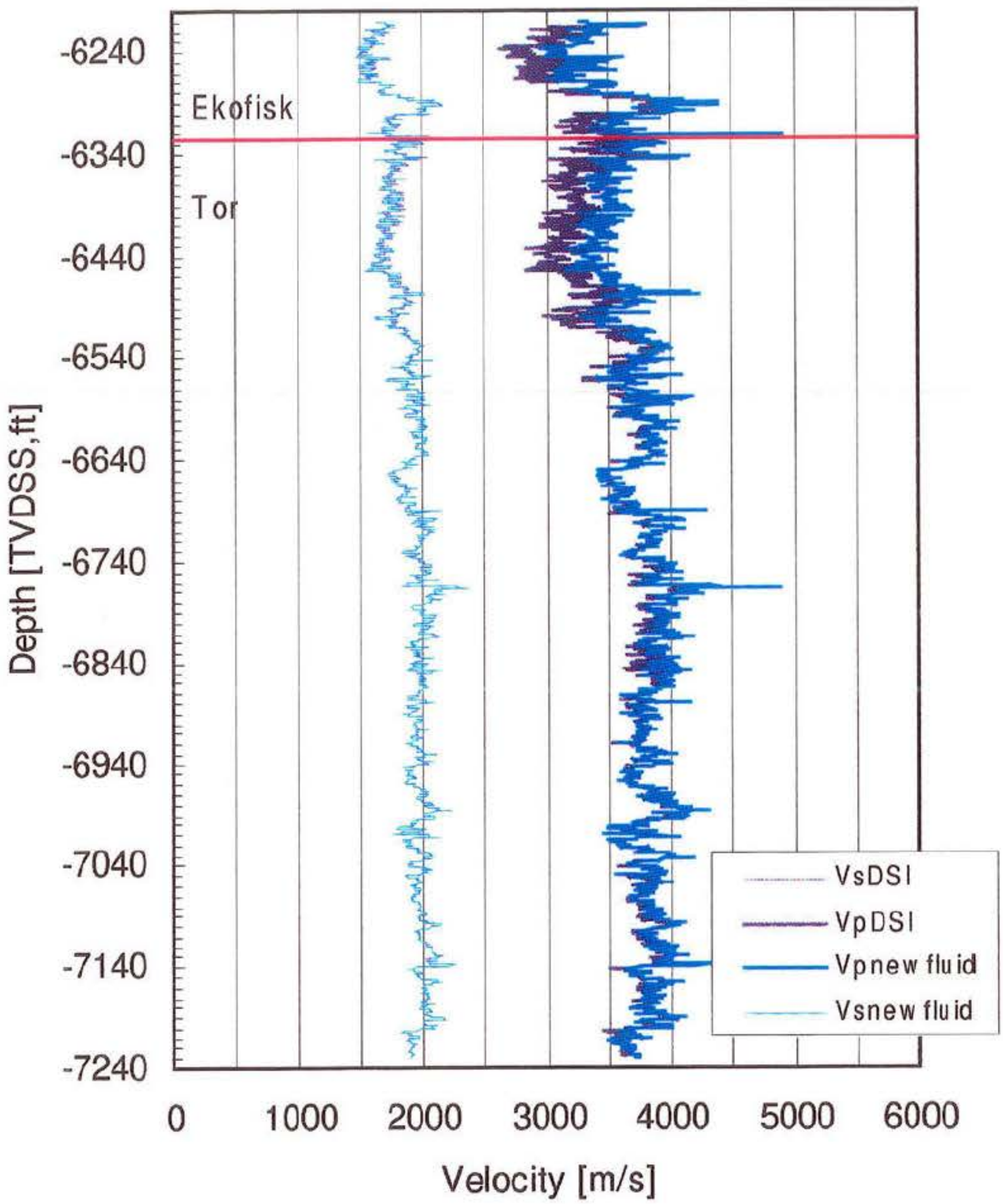

Figure 16. V_p and V_s vs. depth for well MFF-19P. Acoustic response of rock saturated with substituted fluid (Sw=100%, light blue signature). Original response included.

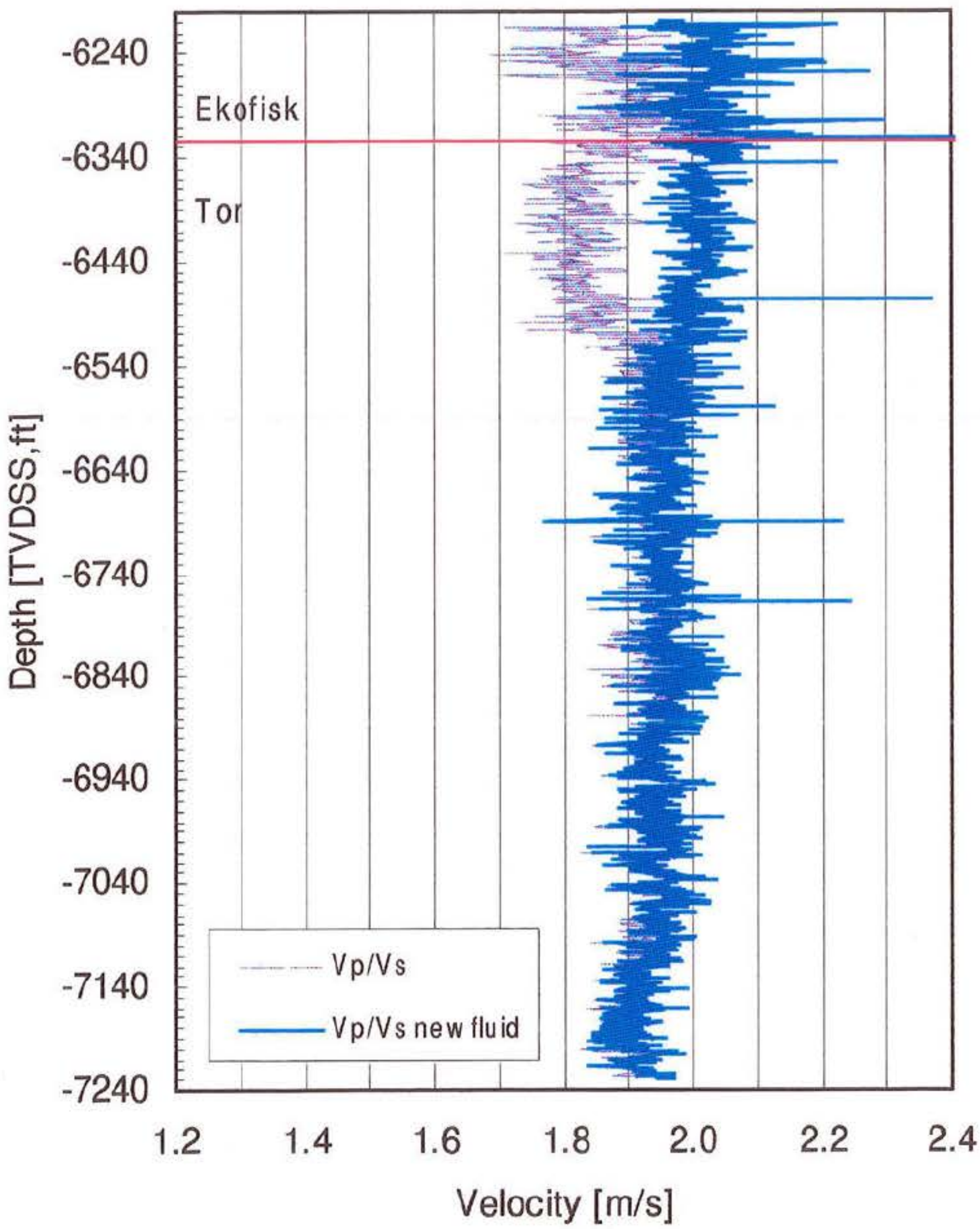

Figure 17. V_p/ V_s vs. depth for well MFF-19P. Acoustic response of rock saturated with substituted fluid (S_w=100%), light blue signature). Original response included.

(Appendix 3 continued)

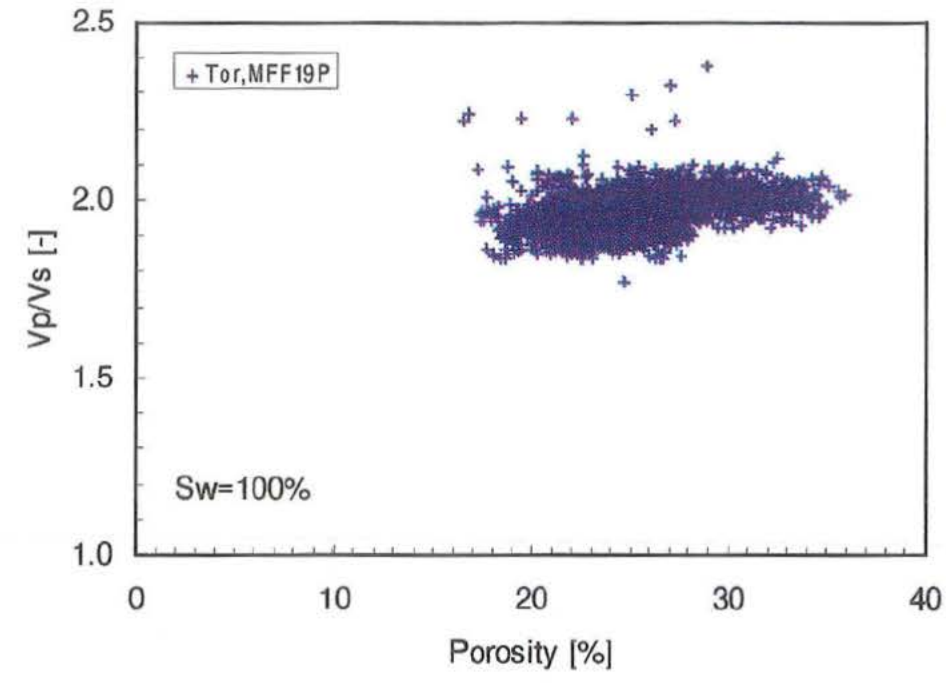

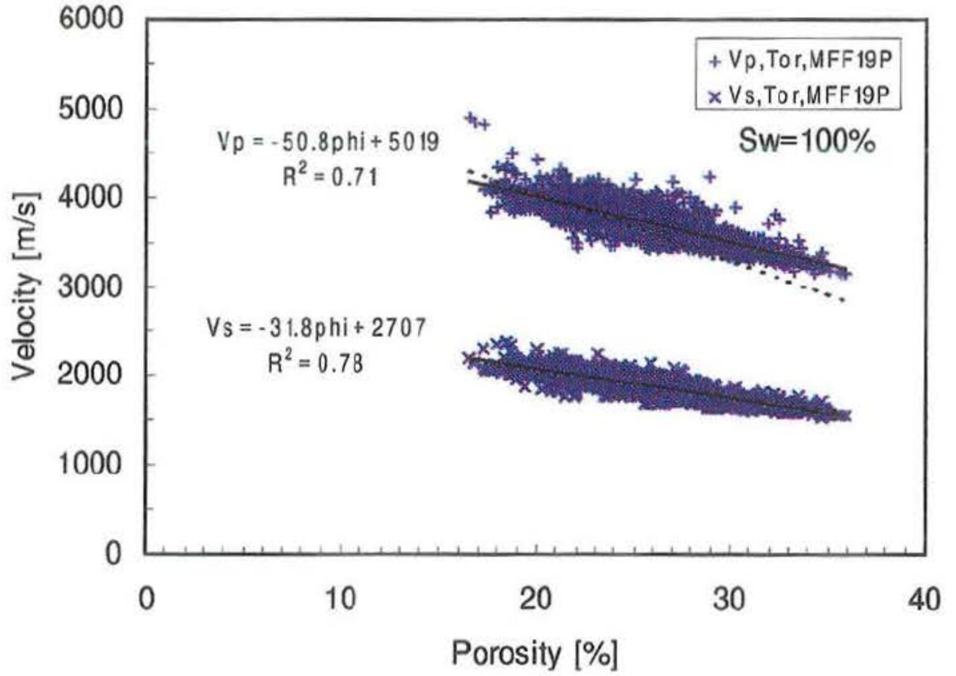

Figure 18 (top). V_p / V_s vs. porosity for Tor Formation, well MFF-19P. Acoustic response of rock with substituted fluid (S_w=100%) [no. of points: 3396].

Figure 19 (bottom). V_p and V_s vs. porosity for Tor Formation, well MFF-19P. Acoustic response of rock with substituted fluid (S_w=100%) [no. of points: 3396]. Linear trend of Figure 8 is included (dotted line signature).

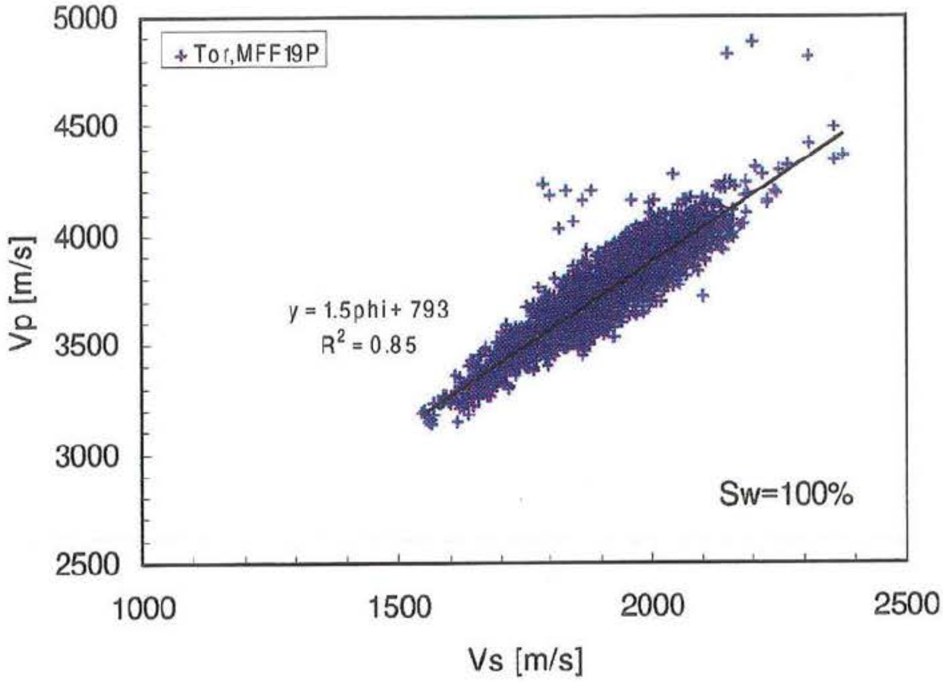

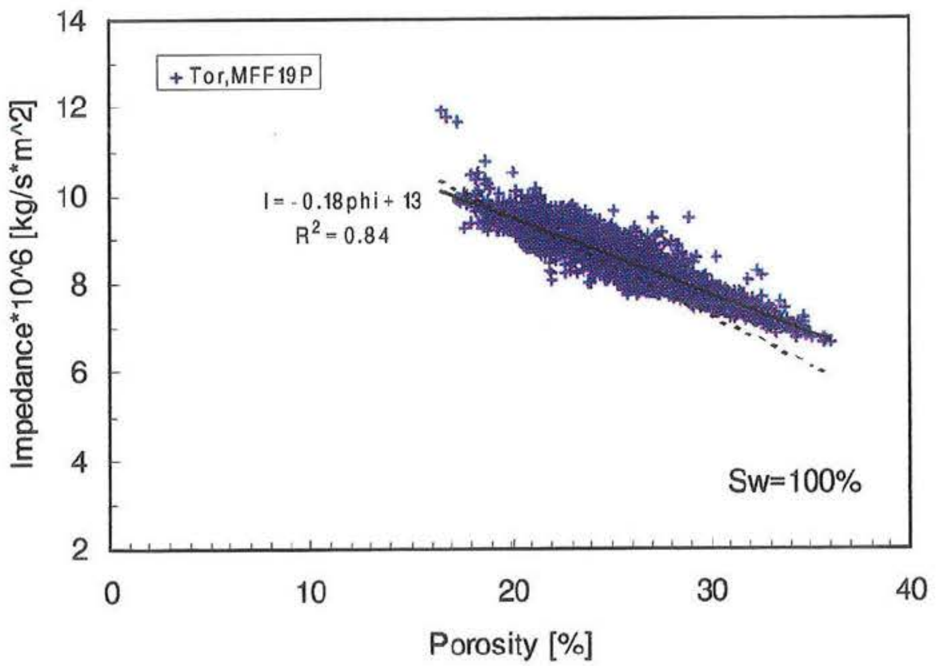

Figure 20 (top). V_p vs. V_s for Tor Formation, well MFF-19P. Acoustic response of the rock with substituted fluid (S_w=100%) [no. of data points 3396].

Figure 21 (bottom). Impedance (V_p *ρ) vs. porosity for Tor Formation, well MFF-19P. Response of the rock with substituted fluid (S_w=100%) [no. of data points 3396]. Linear trend of Figure 13 is included (dotted line signature).